Proceedings of the 2023 International Conference on Mechatronics and Smart Systems
DOI: 10.54254/2755-2721/10/20230167

Real-time path planning based on improved artificial potential field method

Guangyi Wang

Tandon School of Engineering, New York University, 6 MetroTech, Brooklyn, NY, 11217, United States.

gw2315@nyu.edu

Abstract. Nowadays, with the development of robotics-related technology, its applications permeate many aspects of work and life; In product manufacturing and assembly, tech companies switch from manual to robot automation which improves the production volume and reduces the assembly time. In the tertiary sector including health and social work, the robots learn how to interact with people to meet specified requirements. Path planning constitutes a critical module of robotics engineering that aims to provide the optimal solution for the robot to reach its target point. The artificial potential field methods, refers to APF, are widely used to realize path planning due to their simplicity of calculation and effectiveness in obstacle avoidance. However, the traditional artificial potential field method features the local minimum and oscillation, and unreachable target point problems that make it hard for robots to reach the target point. Based on the weaknesses, an improved version of the gravitation and repulsion force function was introduced in this paper. In addition, the concept of safety distance also contributed to the path planning for robots. Through the simulation experiment, it was shown that the improved APF algorithm successfully addressed the local minima and unreachable target point problem, which could navigate robots to arrive at the destination in both 2D and 3D space by avoiding collision with obstacles.

Keywords: robots, improved artificial potential field method, local minima, oscillation, unreachable target point.

1. Introduction

The diverse research topics in the functionality and potential application of robotics attracted scientists and engineers from different backgrounds to work together. One of the most inspiring directions in robotics engineering that has a long history is the path planning method research of the moving object in 2D or 3D space. The core objective of path planning lies in determining a sequence of movement that could manipulate the robots starting from the initial position to safely and effectively reach the desired target point in the complex environment without colliding with any obstacles or other robots [1]; The global and local path planning are two subdivisions that use different strategies to realize the path planning [2]. Global path planning takes advantages of the information in a given environment and implemented algorithms such as$A$*, colony, and Randomly Exploring Random Tree (RRT) to find the optimal path [3-5]. Local path planning focused on generating a feasible path in the immediate vicinity of the robot, which could be achieved by the artificial potential field (APF), pure pursuit, and model

DOI: 10.54254/2755-2721/10/20230167

predictive control method (MPC) that could adapt to dynamic changes in the surrounding environment [6]. Compared with other complicated algorithms, the artificial potential field method is more user-friendly for path planning based on its simple calculation and hands-on simulation. Nevertheless, the traditional artificial potential field presents challenges in situations where the local minimum problem or unreachable target point occurs [7]. The local minimum problem is when the robots experience zero net force in the 2D or 3D complex environment, which keeps the robot static and away from the desired target point. The unreachable target point means that the robots experienced gravitational attraction weaker than the repulsive force exerted by the obstacles surrounding the robots. The entire path planning simulation will be therefore interrupted if one of these two scenarios happens. The optimal solution to improve the traditional artificial potential field method is still a topic of discussion and open to different interpretations from researchers. Yifan Su et al. designed a simulated annealing method that utilized the metropolis criteria to solve the local minimum and oscillation problem [8]. Chengfu Jiang proposed the concept of an escaping force that can be used to adjust the gravitational attraction and repulsion force in the vertical direction, thereby enabling the robot to escape away from local minima points [9]. Xia Chen developed a path optimization technique that iteratively determines the optimal solution for every single point along the path [10].

The aim of this research is to address the limitations of the traditional artificial potential field (APF) method, specifically the issues related to local minima and unreachable target points. This will be achieved by modifying the parameters and safety distance criterion of the gravitational and repulsive force functions used in the APF method. Additionally, a flowchart diagram will be established to provide a clear outline of the steps required to implement the improved APF algorithm.

The structure of this research paper is divided into three main parts. Firstly, the traditional artificial potential field approach is presented, with its limitations highlighted. Secondly, an improved APF algorithm is proposed to address the issues of local minima and unreachable target point. Lastly, the simulation results are analyzed and compared with these of the traditional artificial potential fields.

2. Concept of traditional artificial potential field (APF) method

In 1986, Oussama Khatib, currently a roboticist and computer science professor from Stanford University, proposed the traditional artificial potential field method [11]. The approach assumes that a mobile robot or unmanned aerial vehicle (UAV) within a given workspace is subject to an attraction force generated by the final target point, which acts as a gravitational field; At the same time, the robot experiences the repulsion force from the surrounding obstacles in the workspace; The gravitational attraction and repulsion force finally combine into the resultant force in 2D or 3D cartesian coordinates, which eventually navigates the robot to reach the destination. Figure 1 describes the free-body diagram of robots in the potential field:

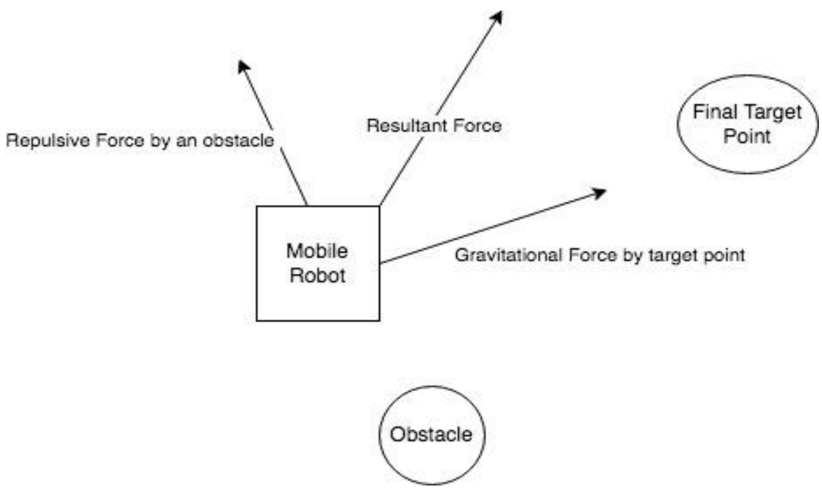

Figure 1. Free body diagram of mobile robot in the workspace.

DOI: 10.54254/2755-2721/10/20230167

2.1. Basic gravitational field and force function are defined as:

$$U_{att}(X) = K_{att}(X_u - X_g)^2 \tag{1}$$

The equation involves several parameters. K_{att} represents the dynamic gain coefficient of attraction force, X_u is the coordinate of the moving object such as mobile robot or UAV, X_g is the coordinate of the destination point, and the Euclidean or absolute distance between the mobile robot and destination point is given by $(X_u - X_g)^2$.

Gravitational force is obtained by:

$$F_{att} = -\nabla U_{att}(X) = -K_a|X - X_g| \tag{2}$$

Where ∇ is the gradient sign equivalent to the partial derivative of gravitational attraction with respect to the xyzpositions $\frac{\partial U_{att}}{\partial X}, \frac{\partial U_{att}}{\partial Y}, \frac{\partial U_{att}}{\partial Z}$.

2.2. Basic repulsive field and force function are defined as:

The repulsive field generated by obstacles is a function of the distance between the robot and obstacles. When the distance is beyond a certain influential radius, then the mobile robot is considered to be in a relatively safe position, and the repulsive field is zero at that point.

$$U_{rep}\ (x) = \begin{cases} k_{rep}\left(\frac{1}{(X_u - X_{ob})} - \frac{1}{\rho_0}\right)^2, & (X_u - X_{ob}) < \rho_0 \\ 0\ , & (X_u - X_{ob}) \geq \rho_0 \end{cases} \tag{3}$$

Where k_{rep} represents the repulsion force gain coefficient, X_u is the position of the mobile robot/UAV, X_{ob} is the position of the obstacle, ρ_0 is the influential radius of the obstacle.

Gravitational attraction is obtained by:

$$F_{rep} = -\nabla U_{rep}(X) \tag{4}$$

2.3. Resultant potential field and force function are defined as:

$$U_{total} = U_{att}(X) + \sum_{i=1}^{n} U_{rep}(X)$$

$$F_{total} = F_{att} + \sum_{i=1}^{n} F_{rep} = -\nabla U_{att}(X) - \sum_{i=1}^{n} \nabla U_{rep}(X) \tag{5}$$

By combining the gravitational and repulsive potential fields in a 2D or 3D cartesian coordinate system, a resultant potential field is created. This resultant force determines the direction in which the mobile robots should move as it navigates towards the final target point.

There are multiple obstacles surrounding the robot in the path planning, therefore the resultant force is calculated by the gravitational force and summation of repulsion force at any point where the absolute distance between the robot and obstacles is within the influential radius of obstacles. This approach ensures that the robot's movements are influenced by all obstacles in the area of close proximity.

However, here are some disadvantages of using the traditional artificial potential field method for path planning in 2D or 3D space.

2.4. Local minima point

The problem of being trapped in a local minima occurs when the gravitational attraction and repulsion force experienced by the mobile robot cancel each other out in a 2D or 3D coordinate system, leading to the zero resultant force that prevents the robot from reaching the target. This typically happens in situations where an obstacle is located exactly between the robot/UAV and target point. In a virtual

DOI: 10.54254/2755-2721/10/20230167

environment having multiple static and dynamic obstacles, the incidence rate of the local minimum point would be enhanced. Figure 2. depicts two possible situations where the local minimum point may occur:

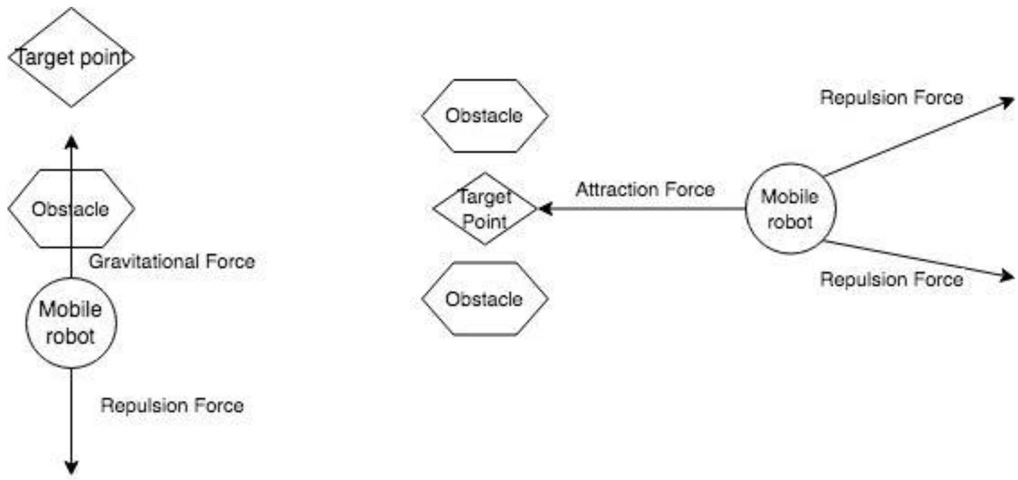

Figure 2. The schematic of situations where the local minimum point may occur.

2.5. Unreachable target point

According to the force function of the traditional APF method, the gravitational force that acts on the robot decreases as it approaches to the target point. Conversely, the repulsive force exerted by obstacles increases as the robot approaches the target point. When an obstacle is situated near the target point, the repulsive force can become greater than the gravitational force, preventing the robot from reaching its destination. In the artificial potential field approach, gravitational attraction and repulsive force are the primary factors that determine the robot's movement. Figure 3. shown below illustrates a scenario where the target point is unreachable:

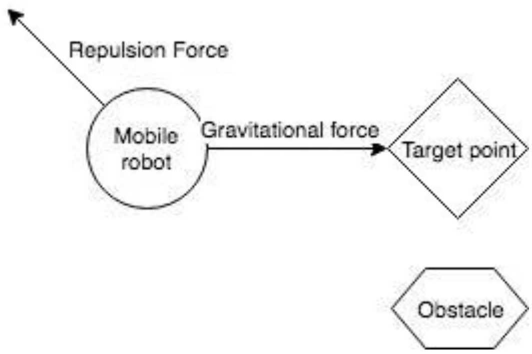

Figure 3. The schematic of the unreachable target problem.

In the traditional APF method, the gravitational and repulsive forces are primarily determined by the distances between the robot, obstacle, and target point; Such a simple assumption would lead to the problem of a local minima and unreachable target. To solve these two issues, the traditional attraction and repulsion force functions were improved to include newly defined force parameters. Within a certain range of safety distances, the adjusted gravitational and repulsive force parameters will be activated in the function to help navigate the robot.

3. Improved APF algorithm

The traditional APF algorithm's force functions result in weaker gravitational force as the robot approaches the final target point and stronger repulsion force as the robot approaches obstacles. Consequently, when obstacles are located close to the target point, the repulsion force may overpower the gravitational force, leading to an imbalanced force that traps the robot in a loop around the target. To tackle this problem, the redefined function aims to address the issue of the unreachable target point.

Improved gravitational field:

$$U_{att}(X) = \frac{1}{2} k_{att} \eta (X_u - X_g)^2$$
$$\eta = \begin{cases} \frac{1}{2}[sin(\frac{(X_u - X_g) - R_0}{\rho_0} \cdot \pi - \frac{\pi}{2}) + 1], & R_0 \leq (X_0 - X_u) < R_0 + \rho_0 \\ 1, & (X_0 - X_u) \geq R_0 + \rho_0 \end{cases} \tag{6}$$

Where k_{att} is the gravitational force gain coefficient, η is the newly defined dynamic attraction coefficient that adjusts the attraction force to avoid zero potential point, X_u is the coordinate of the robot, X_g represents the target coordinate, $(X_u - X_g)^2$ is the Euclidean or absolute distance from the robot to the target, R_0 is the radius of the obstacle, ρ_0 is the influential radius of the obstacle, X_0 is the coordinate of the potential local minima point.

The strength of the gravitational force in the improved APF is dependent t on three main factors: the gain coefficient of attraction force k_{att}, line segment distance from the robot to the obstacle $(X_u - X_g)^2$ and dynamic attraction coefficient η. The value of the dynamic attraction coefficient η changes based on the proximity of the robot to the zero potential point.

The cause of an unreachable target point can be attributed to the final target point not being the local minimum point. To address this issue, a revised gravitational force function is utilized to steer the robot away from the local minima and arrive at the target point where the resultant force is zero. If the distance from the mobile robot and zero potential field point fall in the distance range $R_0 \sim R_0 + \rho_0$, then the newly defined attraction coefficient η would be added into the function to adjust attraction force and keep robots away from local minima. Otherwise, the attraction coefficient η would be equal to unity, remaining the gravitational force function the same as that of the traditional method. In this way, the dynamic gravitational parameter η serves as a decent solution to the local minima problem.

Improved gravitational force:

$$F_{att} = -\nabla U_{att}(X) = -K_{att} \eta (X_u - X_g) \tag{7}$$

The gravitational force is obtained by computing the rate of change of gravitational potential field function in 3D space with respect to the xyz direction:

The improved repulsive potential field and force:

$$U_{rep}(X) = -\lambda K_{rep} (\frac{1}{(X_u - X_{ob})} - \frac{1}{\rho_0})^2$$
$$\lambda = \begin{cases} \frac{1}{2}[cos(\frac{(X_u - X_g) - \rho_0}{\rho_0} \cdot \pi) + 1], & \rho_0 \leq (X_0 - X_u) \leq \rho_1 \\ 0, & (X_0 - X_u) \geq \rho_1 \end{cases} \tag{8}$$
$$F_{rep} = -\nabla U_{rep}(X)$$

Where K_{rep} is the repulsive gain coefficient, λ is the newly defined dynamic repulsion coefficient that adjusts the repulsive force to avoid zero potential point, $(X_u - X_{ob})^2$ is the Euclidean or absolute distance from the robot to the obstacles, and $\rho_1 = 2\rho_0$ is the double influential radius of obstacles.

The improved repulsive force is a function of the repulsion gain coefficient K_{rep}, the shortest line distance from the robot to obstacle $(X_u - X_{ob})^2$, and dynamic repulsion coefficient λ.

Under the traditional APF algorithm, as the robot approaches the final destination, the robot could be directed away from the target due to the strong repulsion force from obstacles. To address this problem, an improved repulsive force function has been introduced. Given the distance from the robot X_u to the obstacle X_{ob} that falls in the specific distance range $\rho_0 \sim \rho_1$, the dynamic coefficient λ is added to the function and changes according to the position of the robot in relation to that of the target

Proceedings of the 2023 International Conference on Mechatronics and Smart Systems
DOI: 10.54254/2755-2721/10/20230167

point; The dynamic coefficient λ eventually becomes zero and turns the repulsion force into zero value when the robot arrives at the target point and stays in a static state. For the second condition of dynamic coefficient λ, it is automatically zero when the robot is out of safety distance from an obstacle.

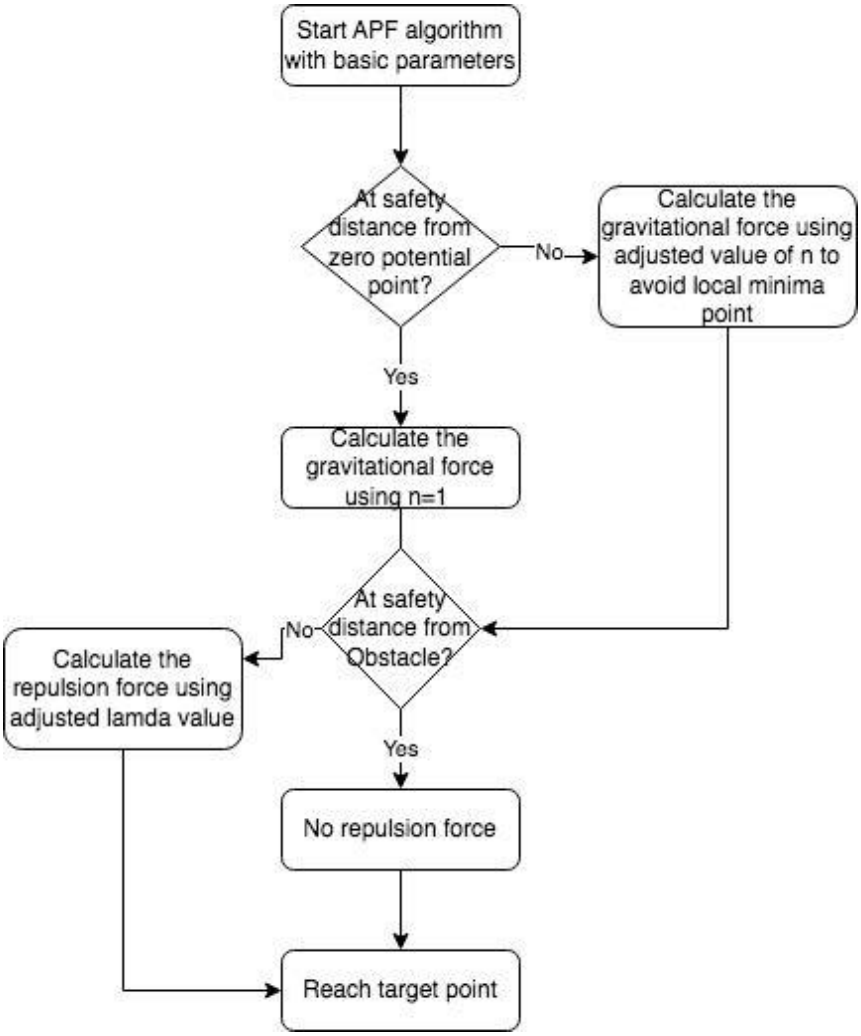

Figure 4. The flowchart diagram for improved APF algorithm.

Figure 4. is the flowchart diagram that clearly shows the steps for implementing APF algorithm. The basic parameter such as the initial, target position, number of obstacles, attraction gain coefficientK_{att}, and repulsion gain K_{rep} were initialized at first. If the mobile robot is close to the local minimum point, the improved gravitational force function is added with the adjusted attraction parameter η for the robot to avoid that point. The improved repulsion force as a function of the robot and target position results in a zero repulsion force at the target point. The new APF algorithm enables the robot to realize path planning by obstacle avoidance.

4. 2D map simulation of both traditional and improved APF method

In path planning simulation research in 2D cartesian space, MATLAB software is used to compare the difference between the traditional and improved APF methods. The objective is to test whether the improved algorithm can successfully solve the problems of local minima and unreachable target point. It turned out that the final simulation results of the improved APF algorithm demonstrated higher capability in the robot's path planning by obstacle avoidance.

DOI: 10.54254/2755-2721/10/20230167

The parameters such as the starting point, end point, and others were first initialized to perform the simulation for the traditional APF algorithm in MATLAB. Table 1. below is a collection of initial parameters:

Table 1. The initialized parameters for the traditional artificial potential field method.

Parameter Name	Symbol	Parameter Value
Starting point coordinate	X_o	(0,0)
Gravitational force gain coefficient	K_{att}	10
Repulsive force gain coefficient	K_{rep}	2
Number of obstacles in the path	n	20
End point coordinate	X_{target}	(10.5,8)
Influential radius of obstacles	ρ_0	20
Number of iterations of force function	J	200
Step Size	I	0.5

In the path planning simulation map shown below, the starting point at (0,0) is set as a red block, the target point at (10.5,8) is set as a red inverted triangle, and twenty obstacles are set as circles. The efficiency of traditional APF algorithms is evaluated based on the robot's motion depicted by a continuous red line.

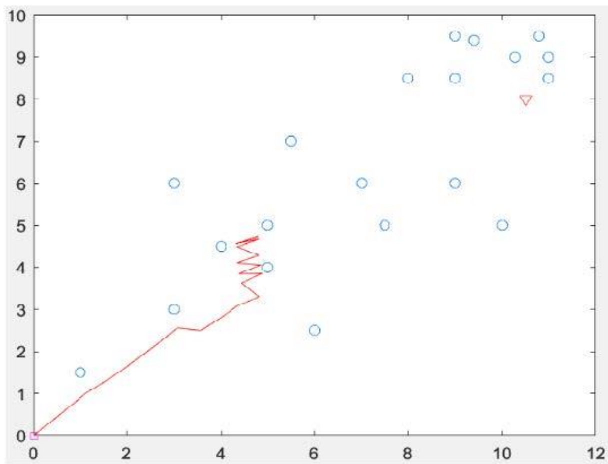

Figure 5. Local minima problem caused by traditional APF.

As shown in Fig. 5 shown above, it is clear that the mobile robot falls into a local minimum point in the position where it is surrounded by two nearby obstacles; Within the influential radius of the obstacles, the robot experiences two repulsion forces that went in the opposite direction and canceled part of each, forming the zero resultant force on the mobile robot. As a result, the mobile robot had local oscillations and failed to reach the final target point.

An improved APF algorithm was utilized to handle the problem of the local minima point; The main approach for the improved APF algorithm focused on adding the dynamic gravitational and repulsive gain coefficient η/λ to the original gravitational force and repulsive force function respectively. The dynamic gain coefficients serve as the functions of the robot, obstacle, target position as well as influential radius ρ_0.

To validate the solution for local minima points, the basic parameters remained unchanged compared with those of traditional APF simulation except for the repulsion gain coefficient K_{rep} The repulsion gain coefficient is 5.

Based on the simulation result of an improved APF algorithm, the mobile robot is in discrete motion represented by small tiny red dots, which is clearly shown in the enhanced picture. Starting point is the red block at the origin, and the ending point is the inverted triangle.

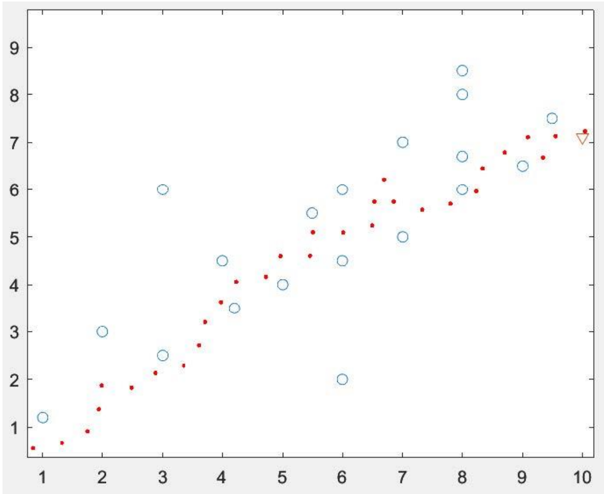

Figure 6. Smooth path planning by improved APF.

From Figure 6 shown above, the mobile robot starting from the origin never stops its motion and finally reaches the designated point by steering away from all the obstacles in the path; The obstacles within the influential radius from the robot apply the adjusted repulsion force on it. Through the simulation, the improved APF algorithm effectively addresses the issue of local minima point by introducing a newly defined dynamic gravitational gain coefficient η.

Besides the local minima problem, the implementation of the traditional APF algorithm faces another challenge called the unreachable target point problem. Below is the simulation result by the traditional APF algorithm.

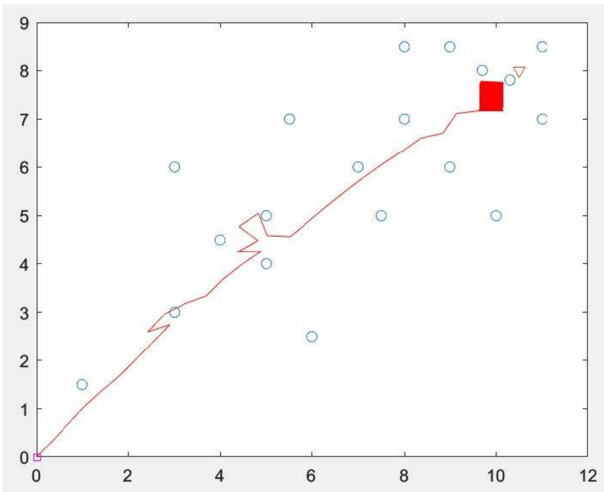

Figure 7. Unreachable target caused by traditional APF method.

The simulation results indicate that as the mobile robot from the origin approaches close to the same final target point (10.5,8) surrounded by the obstacles, it oscillates around the target point and fails to reach it; This is because the repulsion forces from the obstacles become stronger than the gravitational forces as the robot gets closer to the target point. The traditional APF algorithm is therefore not effective in handling the problem of an unreachable target point.

DOI: 10.54254/2755-2721/10/20230167

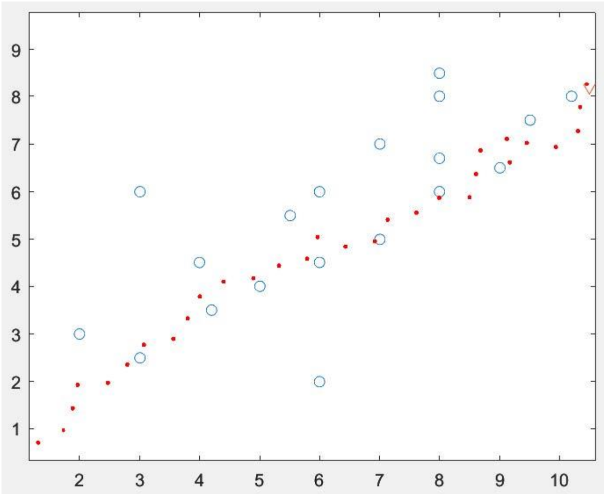

Figure 8. The smooth path planning by improved APF.

The improved APF algorithm can resolve the unreachable target point challenge, as demonstrated in Figure 8. The mobile robot smoothly passes through the obstacle that is placed right in front of the final target point without any collision and reaches the target described by a red inverted triangle. The repulsion force from the obstacle is getting smaller and smaller due to the dynamic repulsive gain coefficient λ added to the repulsive force function. It is clear to see how the improved APF algorithm serves as a solution to the unreachable target points.

Through the 2D path planning simulation conducted in MATLAB, a clear comparison between the traditional and improved APF algorithms in terms of their ability to address local minimum and unreachable target point problems has been presented. Based on the simulation results, it can be inferred that the improved APF algorithm is a more potent and efficient approach for obstacle avoidance and robot navigation.

5. 3D map simulation of both traditional and improved APF method

In the map shown below, the dimension of the 3D space is (100,100,100). The starting point at (0,0,0) is set as the red star, the target point at (40,40,40) is set as an inverted triangle, and six obstacles along the path are set as circles. The motion of the robot is described by the continuous red line. Below are four figures representing four difficulty levels of path planning for the robots. The first three figures successfully demonstrate the efficacy of the improved APF algorithm in path planning. However, the last figure shows the current improved APF algorithm may encounter difficulties when the environment is getting intensively complicated.

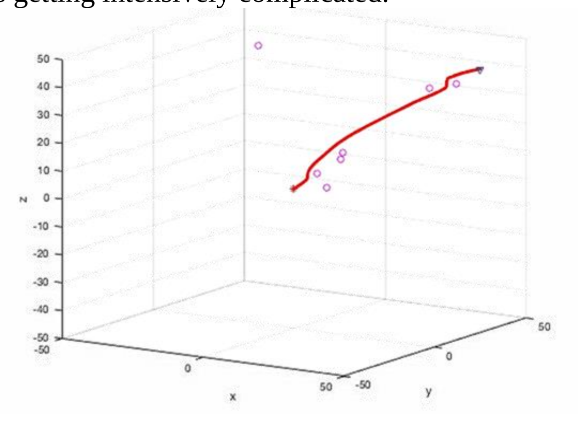

Figure 9. Smooth 3D path planning by improved APF.

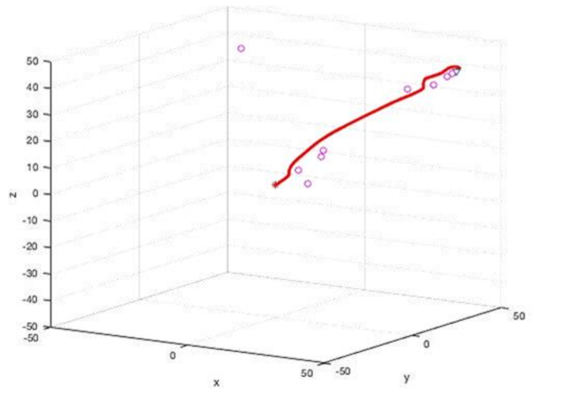

Figure 10. Smooth 3D path planning by improved APF.

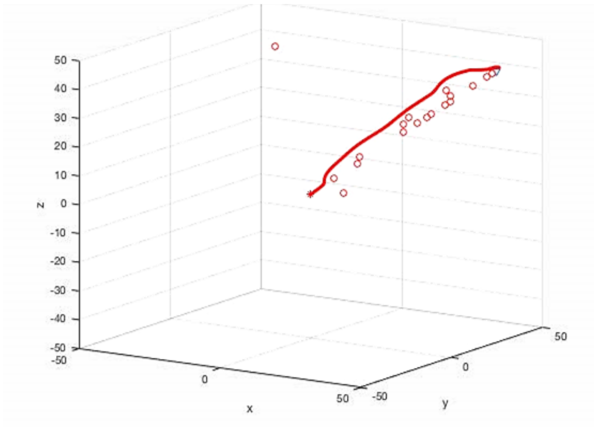

Figure 11. Smooth 3D path planning by improved APF.

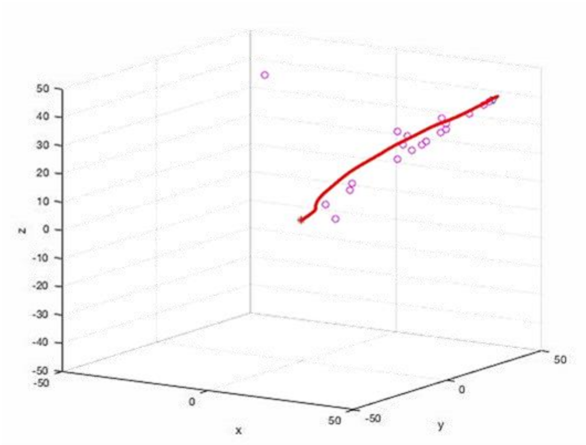

Figure 12. Path planning failure by improved APF.

The mobile robot navigates smoothly to the final target point without encountering any obstacles as shown in Figure 9. In Figure 10, the number of obstacles close to the final target point is increased from two to four, yet the robot can still efficiently reach the final destination. The effectiveness of the path planning approach using the improved APF algorithm is strongly demonstrated in Figure 11, where the robot successfully bypasses all the obstacles and reaches the target position. However, Figure 12 reveals a limitation of the improved APF algorithm, as it fails to guarantee perfect path planning when there are too many obstacles in the path toward the target point.

6. Conclusion

This research paper mainly proposed the improved APF method and analyzed its performance in solving the local minima and unreachable target point problems compared with that of the traditional APF algorithm. The 2D and 3D simulation results were demonstrated in the MATLAB simulation respectively. Based on the MATLAB simulation, it can be concluded that the improved APF algorithm outperformed the traditional one in the robot's path planning through obstacle avoidance. However, if the environment setting becomes extremely complicated as shown in Figure 13., the improved APF algorithm may exhibit certain shortcomings and guide the robot in the wrong direction. Therefore, it still requires deeper insight from researchers to handle more complex scenarios and make it more robust and reliable for the path planning task.

References

[1] Q. Liu, J. Liu, Y. Zhao, R. Shen, L. Hou, and Y. Zhang, 2022 "Local path planning for multi-robot systems based on improved artificial potential field algorithm," *in 2022 IEEE 5th Advanced Information Management, Communicates, Electronic and Automation Control Conference (IMCEC)*, vol. 5. IEEE, pp. 1540–1544.

[2] Y. Li, B. Tian, Y. Yang, and C. Li, 2022 "Path planning of robot based on artificial potential field method," *in 2022 IEEE 6th Information Technology and Mechatronics Engineering Conference (ITOEC)*, vol. 6. IEEE, pp. 91–94.

[3] F. Li, Z. Huang, and L. Xu, 2019 "Path planning of 6-dof venipuncture robot arm based on improved a-star and collision detection algorithms," *in 2019 IEEE international conference on robotics and biomimetics (ROBIO)*. IEEE, pp. 2971–2976.

[4] O. Erkut and F. Hardalac¸, 2021 "Comparison of ant colony optimization and artificial bee colony algorithms for solving electronic support search dwell scheduling problem," *in 2021 15th Turkish National Software Engineering Symposium (UYMS)*. IEEE, pp. 1–6.

[5] B. Wan, Y. Qin, and W. W. Song, 2018 "Path planning strategy of mobile nodes based on improved rrt algorithm," *in 2018 3rd International Conference on Computational Intelligence*

and Applications (ICCIA). IEEE, pp. 228–234.

[6] P. V. S. Reddy, 2021 "Generalized fuzzy logic with twofold fuzzy set: learning through neural net and application to business intelligence," *in 2021 International Conference on Fuzzy Theory and Its Applications (iFUZZY)*. IEEE, pp. 1–5.

[7] Y. Sun, W. Chen, and J. Lv, 2022 "Uav path planning based on improved artificial potential field method," *in 2022 International Conference on Computer Network, Electronic and Automation (ICCNEA)*. IEEE, pp. 95–100.

[8] N. He, Y. Su, X. Fan, Z. Liu, B. Wang et al., 2020 "Dynamic path planning of mobile robot based on artificial potential field," *in 2020 International Conference on Intelligent Computing and Human-Computer Interaction (ICHCI)*. IEEE, pp. 259–264.

[9] C. Jiang, Y. Gao, and P. Yang, 2021 "Mobile robot obstacle avoidance based on improved artificial potential field method," *in 2021 3rd International Conference on Robotics and Computer Vision (ICRCV)*. IEEE, pp. 18–23.

[10] X. Chen and J. Zhang, 2013 "The three-dimension path planning of uav based on improved artificial potential field in dynamic environment," *in 2013 5th International Conference on Intelligent Human-Machine Systems and Cybernetics*, vol. 2. IEEE, pp. 144–147.

[11] O. Khatib, 1986 "Real-time obstacle avoidance for manipulators and mobile robots," *The international journal of robotics research*, vol. 5, no. 1, pp. 90–98.